Sensors & Diagnostics

Supplementary information

A lab-on-a-chip system integrating DNA purification and loop-mediated isothermal amplification for the quantification of toxic diatom *Pseudo-nitzschia multistriata*

Authors: Ahmed I. Alrefaey, Jonathan S. McQuillan, Allison Schaap, Fabrizio Siracusa, Christopher L. Cardwell, John Walk, Daniel Rogers, Reuben Forrester, Matthew C. Mowlem and Julie C. Robidart

Correspondence: Ocean Technology and Engineering, The National Oceanography Centre, European Way, Southampton, UK, SO14 3ZH. Email: j.robidart@noc.ac.uk, Telephone: +443001312594

Table of Contents

Part I: DNA Extraction Methods and Performance

S1. Quality verification of DMA-based extraction techniques

The DMA extraction protocol was evaluated for the extraction of DNA from a variety of sources, including Eukaryotic cells (*Pseudo-nitzschia* diatom *spp*), Bacteria (*Escherichia coli*) and Dinoflagellates (*Alexandrium minutum*). The *Pseudo-nitzschia* cells were grown as previously described in section 2.1 of the main article. *A. minutum* CCAP 1119/15 was grown in L1 medium. [1] *A. minutum* cells were enumerated and grown at the same incubation conditions as *Pseudo-nitzschia,* as detailed in section 2.1 of the main article. The bacterial strain used in this study was *Escherichia coli* NCTC9001 type strain (*E. coli*) that was obtained from the UK National Collection of Type Cultures (NCTC). *E. coli* cells were counted as described. [2, 3] Cells were harvested by centrifugation at 7,100 rpm for 5 minutes at 4°C and stored at -80°C until further processing, with the same protocol applied to samples for both the kit and DMA extractions to ensure any cell lysis effects were equivalent. Each replicate cell pellet was processed into the microfluidic chip to perform the same DMA extraction protocol as described in section 2.4.1 of the main article. DNeasy Mini Kit (Qiagen), DNeasy Plant Pro Kit (Qiagen), and GenElute Bacterial Genomic DNA Kit (Sigma-Aldrich) were used as standard methods to extract DNA from *P. multistriata*, *A. minutum*, and *E. coli* cells, respectively. The DNA recovery efficiencies from the commercial kits were averaged for comparison with the DMA-based techniques. For a bead-free control, glass fiber membranes (GF/F grade, Whatman™) were laser-cut to match the extraction-chamber layout using a CO_2-based cutter (Speedy 100, Trotec Laser GmbH, UK) and subsequently treated with ozone and APTES (as described in Section 2.3.2, the main text). We evaluate the extraction capabilities of two different silica substrates, incorporating beads and glass fibre membrane, against the

commercial extraction kits. The absolute extraction efficiency was calculated using the formula: Extraction Efficiency (%) = (C × V/ DNA input) × 100, where C is the concentration of DNA in the extract (ng/L), V is the total volume in µL), and DNA input refers to starting DNA based on cell count and known DNA mass per cell. [4, 5]

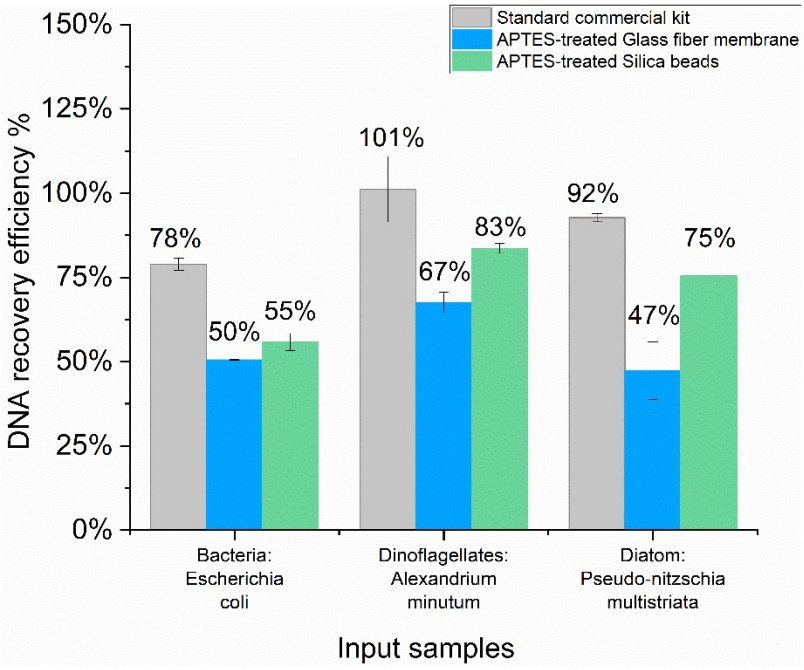

Supplementary Figure S1. Performance assessment of DMA-based method for DNA extraction from various samples. The DNA capture efficiency was evaluated by comparing the proposed DMA microfluidic method using silica beads and glass fibre paper with the reference extraction by widely used kits processing the same volume of sample.

The silica beads delivered higher DNA recovery compared to the membrane, irrespective of the sample type (Figure S1). For example, the recovery using silica beads was 55%±2.51 versus 50%±0.13 for *E. coli*, 83%±1.47 versus 67%±3.05 for *A. minutum*, and 75%±3.86 versus 47%±8.61 for *P. multistriata.* The capture of *P. multistriata* DNA on silica beads was approximately 75%±3.86, which is lower than recovery from the DNeasy Mini Kit (Qiagen) (92%±1.22). For the Dinoflagellate *A. minutum*, DNA recovery was 83%±1.47 using silica beads, lower than the DNA recovery of DNeasy Plant Pro Kit (Qiagen) (101%±9.71). Recovered DNA concentrations from *E. coli* were 55%±2.51 using silica beads vs. 78%±1.77 recovery

using the GenElute Bacterial Genomic DNA Kit (Sigma-Aldrich). DNA extracts of *P. multistriata* showed purity ratios (260/280) below the optimal value of approximately 1.8, as illustrated in Figure 3A (main text). These purity values correspond with Qubit measurements of 7.38 ± 0.14 and 5.12 ± 0.33 ng/µL, indicating low DNA levels rather than contamination. When extracting serial dilutions of *P. multistriata* from 10 to 10^5 cells/mL on-chip, low-purity DNA samples did not inhibit LAMP amplification in independent experiments. The LAMP time-to-threshold (Tt) was consistent, showing that sensitivity is unaffected by residual contaminants in DNA elutes, as shown in Supplementary Figure S5.

S2. Optimisation of the DNA extraction module.

The optimisation of the DNA extraction module in LAMPTRON is described in Section 2.4.1 of the main text, where reagent volumes and flow rates were optimised using fluid control via solenoid valves (LFNA1250325H, The Lee Company, Connecticut, U.S.A.) and programmable syringe pump (Harvard Apparatus, Holliston, United States).

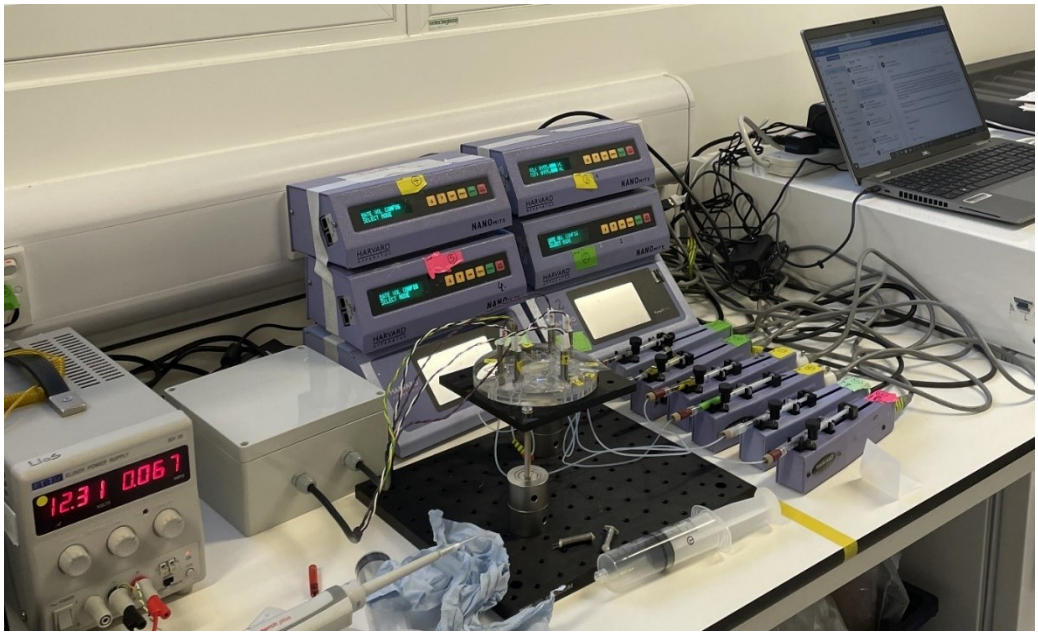

Supplementary Figure S2. Optimisation of the DNA extraction module in LAMPTRON was conducted using a new transparent PMMA-built chip. Parameters such as reagent volumes, flow rates, and diffusion times were optimised within this experimental setup. Solenoid-operated valves were fixed on the test chip, which was connected to syringe pumps for controlled injection of samples and reagents, controlled via a Windows-based software.

S3. Oxygen plasma treatment of silica beads

The oxygen plasma treatment process used to activate the silica bead surfaces is described in Section 2.3.2 of the main text, and was carried out prior to packing the beads into the extraction microchamber of the microfluidic chip.

Supplementary Figure S3. Silica beads underwent oxygen plasma treatment to activate the surface silanol groups, employing a plasma activation system (Diener Electronic, Ebhausen, Germany). The effectiveness of the plasma treatment was assessed by observing the behaviour of water droplets on the beads. Resistance to wetting by beads indicated successful plasma treatment [6].

S4. Comparison of extraction reagent costs

This section presents a cost comparison of extraction reagents, demonstrating the economic advantage of the LAMPTRON method over conventional commercial kits.

Supplementary Table S1. Cost comparison for reagents between LAMPTRON extraction and Qiagen commercial methods.

Items Description	Component	Cost (£), inc. VAT per sample	Manufacturer	Product Number
Current extraction DMA-based method:	2% APTES (aminopropyl triethoxysilane)	0.0061	Sigma-Aldrich	741442-100ML
	95% Ethanol	0.0045	Sigma-Aldrich	652261
	0.1 M Tris-HCl (pH 8.0)	0.0023	SERVA	39792.01
	10 mM EDTA	0.0085	Invitrogen	15575-038
	1% sodium dodecyl sulfate (SDS)	0.0054	Sigma-Aldrich	L4390-100G
	10% Triton X-100	0.0033	Sigma-Aldrich	93443-500ML
	0.1 mg/mL Proteinase K	0.000014	Qiagen	56304
	100 mg/mL Dimethyl adipimidate (DMA)	0.069	Alfa Aesar	L10515.09
	0.01 M Phosphate-buffered saline (PBS)	0.00035	Sigma-Aldrich	P4417-100TAB
	0.1 M Trisodium citrate		Alfa Aesar	45558
	10 mM sodium bicarbonate	0.00078	Sigma-Aldrich	S7277-250G
	Glass beads	0.0082	Sigma-Aldrich	G1152-100G
	DEPC-treated water	0.0054	Thermo Fischer	R0601
Total cost per sample	£0.11			
Qiagen extraction method	DNeasy Plant Mini kit	4.18	Qiagen	69104
Total cost per sample	£4.34			

Part II: LAMP Assay Development and Quantification

S5. Development of LAMP isothermal assay

The gene of interest is a cytochrome P450 homologous to *dabD*, which is implicated in domoic acid (DA) biosynthesis in *Pseudo-nitzschia spp.*[7-9] Cytochrome P450 enzymes are a superfamily of enzymes that are involved in the oxidative metabolism of a wide range of compounds, including drugs, xenobiotics, and endogenous substances such as fatty acids and steroids. [10] Importantly, its role in DA biosynthesis was confirmed through transcriptomic [11, 12] and sequence analysis of the cytochrome P450 *dabD* gene in toxin-producing *Pseudo-nitzschia spp* [8], as well as functional assays indicating that cytochrome P450 DabD catalyses a key oxidative step in the DA biosynthetic pathway. [7, 9]

BLAST analysis was performed using the published *dabD* gene sequence [7] from *Pseudo-nitzschia multistriata* as the query. The sequence was searched against publicly available nucleotide (nt) database of the National Centre for Biotechnology Information (NCBI) (https://www.ncbi.nlm.nih.gov/) (accessed March 14, 2022) to identify homologous *dabD* sequences suitable for primer design. [13] The search was performed using BLASTn with the following parameters: E-value cutoff = 0.05-0.1, match/mismatch scores = 2-3, word size = 7-28, gap existence cost = 5, extension cost = 2, and a threshold of 1-100 hits per query. This target sequence was then searched across available *P. multistriata* genomes in public databases such as the SZN institute database (https://bioinfo.szn.it/), the Earlham Institute's database (http://apollo.tgac.ac.uk/),[14, 15], and the Ensemble database (https://protists.ensembl.org/) (accessed March 14, 2022). In total, 8 BLAST hits with ≥ 80% query coverage were retrieved when querying the *P. multistriata* genome and transcriptome databases using the *dabD* gene as input. These sequences were subsequently aligned using

181 the ClustalW multiple sequence alignment tool (version 2.1) to identify conserved regions
182 suitable for oligonucleotide binding. [16] To validate the accuracy of amplifying the target
183 sequence, additional verification measures were taken as follows: the consensus sequence
184 was subjected to comparison with the reference protein sequences available in the GenBank
185 database using BlastX. [17] Furthermore, protein domains were analysed to examine the
186 translated protein sequence of the target conserved region. [18] The bioinformatics analyses
187 were conducted using either the NCBI website's toolkit or Geneious Prime® v2019.2.3
188 software (Biomatters Ltd, Auckland, NZ).

189 The LAMP oligonucleotides flanked a consensus region of a total of 230 base pairs with a
190 pairwise identity of 76% (Figure S4). Table S1 contains the ID numbers and functional
191 annotations corresponding to the *Pseudo-nitzschia spp.* sequences that were employed to
192 determine the consensus target sequence. The consensus sequence obtained from the
193 alignment analysis was employed for the design of the LAMP assay. The designed
194 oligonucleotides share approximately 77.4% identity with all *P. multistriata* cytochrome P450
195 sequences (Figure S4). Among these, only two cytochrome P450 isoforms have been
196 confirmed in domoic acid biosynthesis: the *dabD* sequence from *P. multistriata* [7], which
197 shares an average of 88% identity with our designed LAMP primers, and the MH202990
198 sequence from *P. multiseries* (NCBI), which shares 79% identity (Figure S4; Table S2). When
199 comparing these two confirmed isoforms (*CYP450* (*dabD*) sequences of *Pseudo-nitzschia*
200 *multiseries* isolate 15091C3 (NCBI Gene ID: MH202990) with those of *Pseudo-nitzschia*
201 *multistriata* [7], pairwise identity was 83.1%. Therefore, both sequences from *P. multistriata*
202 and *P. multiseries* were included in the alignment to generate a consensus sequence.
203 LAMP primers (Table 1) were designed to target six distinct regions of the consensus sequence
204 (Figure S4). Percentage identities for the LAMP primer binding sites were 77.9% for LAMP-

F3, 77.4% for LAMP-B3, 73% for LAMP-FIP, 77.8% for LAMP-BIP, 74.3% for LAMP-LF, and 81.3% for LAMP-LB (Figure S4). To evaluate potential secondary structures among LAMP primers, the Oligo Analyser folding tool (https://eu.idtdna.com/calc/analyzer) and PrimerExplorer™ V5 software (Eiken Chemical Co., Ltd., Tokyo, Japan) were employed with a focus on the 3' end regions, as they are critical in promoting stable binding and elongation during the amplification process, achieving specific LAMP amplification. [19] The selection of potential LAMP primer candidates was guided by a Gibbs free energy (ΔG) threshold of -7 kcal/mol. This criterion was employed to prevent mispriming among the six LAMP primers during the amplification process. [20] Therefore, primer pairs with lower ΔG values, which could result in thermodynamically stable heterodimers and non-specific LAMP products, were excluded. This strategy effectively prevented the formation of heterodimers, thus ensuring efficient and specific LAMP amplification (Figures 4A & 5A in the main article).

To evaluate the specificity of the designed LAMP primers, triplicate no-template control (NTC) reactions were conducted. The assay's specificity was further assessed using genomic DNA samples from a panel of 10 different *Pseudo-nitzschia* species and 8 non-target microalgal strains, as detailed in Supplementary Table S4. All NTCs and non-*Pseudo-nitzschia* samples consistently showed no amplification, indicating the absence of false positives and confirming the high specificity of the LAMP assay. Positive amplification was observed exclusively from *Pseudo-nitzschia* species, indicating selective detection by the LAMP method.

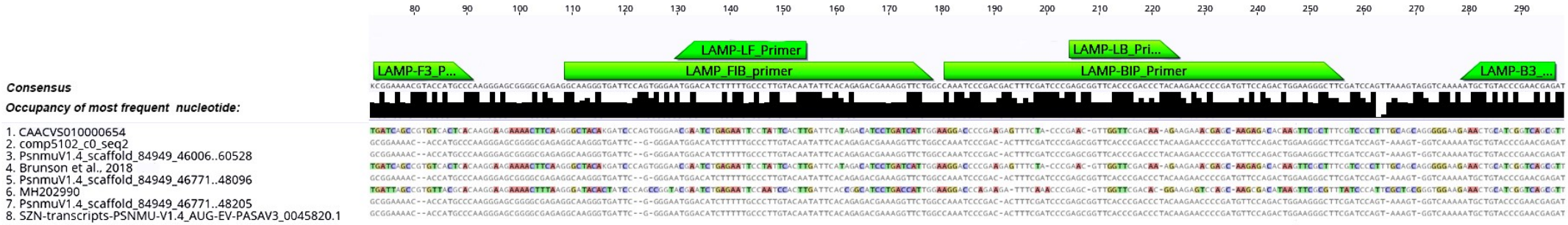

Supplementary Figure S4. Multiple Sequence Alignment of the *Cytochrome CYP450 DabD* gene sequences, revealing binding sites for the oligonucleotides used in the LAMP analysis of *P. multistriata cells*.

Supplementary Table S2. List of *Cytochrome CYP450 DabD* gene sequences obtained from *Pseudo-nitzschia* genomes and the nucleotide percent identification relative to *dabD* from [7].

Species	Strain	Accession Number	Functional annotation	% Identity dabD (relative to [7]	Source
P. multistriata	B856	CAACVS010000654	Cytochrome CYP450	99.8	Ensemble Protists [a]
P. multistriata	B857	PSNMU-V1.4_AUG-EV-PASAV3_0045820.1	Cytochrome CYP450	52.6	SZN [b]
P. multiseries	15091C3	MH202990	*DabD*, Cytochrome CYP450	83.1	NCBI [c]
P. multistriata	N/A	Brunson et al., 2018	*DabD*, Cytochrome CYP450	100	[7]
P. multistriata	B939	PsnmuV1.4_scaffold_84949_46006..60528	Cytochrome CYP450	55.1	[14]
P. multistriata	B936	PsnmuV1.4_scaffold_84949_46771..48096	Cytochrome CYP450	55.1	[14]
P. multistriata	B856	PsnmuV1.4_scaffold_84949_46771..48205	Cytochrome CYP450	55.1	EarlHam [d]
P. multistriata	B936	comp5102_c0_seq2	Cytochrome CYP450	52.6	[15]

[a] Ensemble Protists; European Nucleotide Archive for Protist Genomes, [b] SZN; Genome database of the Stazione Zoologica Anton Dohrn, [c] NCBI; National Centre for Biotechnology Information GenBank, [d] EarlHam; The genome portal of the Earlham institute, UK.

Supplementary Table S3. The hits of BLAST analysis for LAMP amplicon.

				BLASTN		
Species	**Strain**	**Percent Identity**	**E- value**	**Score**	**Accession Number**	**Source**
P. multistriata	B856	100%	6e-35	74	PSNMU_V1.4_AUG-EV-PASAV3_0045820	Ensemble Protists [a]
				BLASTX		
P. multistriata	B856	96.4	2e-34	161	VEU37775	Ensemble Protists [a]
P. multistriata	B856	65.5	1.5e-11	109	VEU41686	Ensemble Protists [a]
P. multistriata	B856	34.2	0.00074	79	VEU45241	Ensemble Protists [a]
P. multistriata	B856	40.7	0.01	70	VEU44693	Ensemble Protists [a]

[a] Ensemble Protists; European Nucleotide Archive for Protist Genomes.

We compared the consensus fragment against ENSMBL Protist genome repository using both BLASTN and BLASTX analysis following default settings (http://protists.ensembl.org/Pseudonitzschia_multistriata/Tools/Blast). The BLASTN results revealed significant homologous matches with the PSNMU_V1.4_AUG-EV-PASAV3_0045820 gene of the Cytochrome P450 in *Pseudo-nitzschia multistriata* (Table S3). Furthermore, BLASTX analysis of a 230 bp consensus sequence revealed that its protein product shares 40.7% with the complete cytochrome P450 DabD protein (Ensemble accession number: VEU44693) from the ENSMBL Protist genome database, validated as the DabD isoform involved in domoic acid biosynthesis in *P. multistriata.* [8] Although the sequence similarity is low, functional annotation and conserved domain features supported its selection as a putative *dabD* homolog for primer design. Despite the limited genetic information available on the species-specific DabD protein in the *P. multistriata* SZN-B954 strain, we extended our investigation to identify the domain composition of the protein of isothermally amplified products of the LAMP assay by using the NCBI tool of the Conserved Domain Database (CDD). [18] The results revealed that the 230 bp consensus sequence displayed an identical domain

structure to the annotated Cytochrome P450 protein under NCBI accession number cl41757. Since cl41757 is one of many cytochrome P450 isoforms and lacks specific annotation linking it to domoic acid biosynthesis, further functional studies are needed to confirm its role in DA production. Nonetheless, domain structure supports classifying our amplified product within the cytochrome P450 family, which includes the DabD isoform previously implicated in DA biosynthesis in many *Pseudonitzschia spp.* [7, 8, 11, 12]

Supplementary Table S4. Selectivity evaluation of the LAMP assay using *Pseudo-nitzschia* species and non-target microalgal strains.

Species	Isolate Accession	LAMP Amplification
Pseudo-nitzschia multistriata	SZN-B954	+
Pseudo-nitzschia multistriata	SZN-B955	+
Pseudo-nitzschia pungens	CCAP 1061/44	+
Pseudo-nitzschia multiseries	NWFSC 713	+
Pseudo-nitzschia multiseries	NWFSC 714	+
Pseudo-nitzschia multiseries	NWFSC 715	+
Pseudo-nitzschia multiseries	ML-54	+
Pseudo-nitzschia multiseries	ML-55	+
Pseudo-nitzschia multiseries	ML-56	+
Pseudo-nitzschia multiseries	ML-59	+
Karenia brevis	CCMP2228	-
Karenia mikimotoi	CCAP 1127/2	-
Alexandrium tamarense	CCAP 1119/25	-
Synechococcus sp	CCAP 1479/9	-
Prorcentrum lima	CCAP 1136/12	-
Alexandrium minutum	CCAP 1119/15	-
Lingulodinium polyedra	CCAP 1121/7	-
Prorcentrum cordatum	CCAP 1136/16	-

S6. Quantification kinetics and standard curve generation

To evaluate the quantitative performance of the LAMPTRON system, standard curves were prepared by plotting threshold times (Tt, min) versus the logarithm of known input concentrations of *P. multistriata* cells ranging from 1.6×10^{5} to 1.07×10^{1} cells/mL. DNA was purified via on-chip extraction, followed by direct LAMP amplification on the LAMPTRON (sections 2.4.1 and 2.4.2 of the main article). Each cell concentration was tested in triplicate. Linear regression analysis was performed using Origin software (OriginLab, Northampton, MA, USA), providing the correlation coefficients (R^2) to assess the linearity of the log-linear relationship. Separate standard curves were constructed for the fresh and preserved reagent conditions to compare performance. The resulting equations, slopes of the regression lines and R^2 values are shown in Figure S5. The slope (m) of the resulting regression was used to calculate amplification efficiencies, expressed as isothermal doubling time (IDT) using the equation (IDT = - 0.301 x m), where m represents the slope of the graph of Tt value plotted against the amount of target DNA/cells and 0.301 corresponds to a twofold change in concentration at 2. [21] Gels were run using endpoint LAMP products, post-amplification (Figure 4B and 5B in the main article). Minor non-specific amplification products were observed in endpoint gel electrophoresis after LAMP reactions due to the accumulation of looped DNA structures and primer artefacts. Real-time fluorescence detection, rather than gel-based confirmation, was used to determine threshold time (Tt) and quantification.

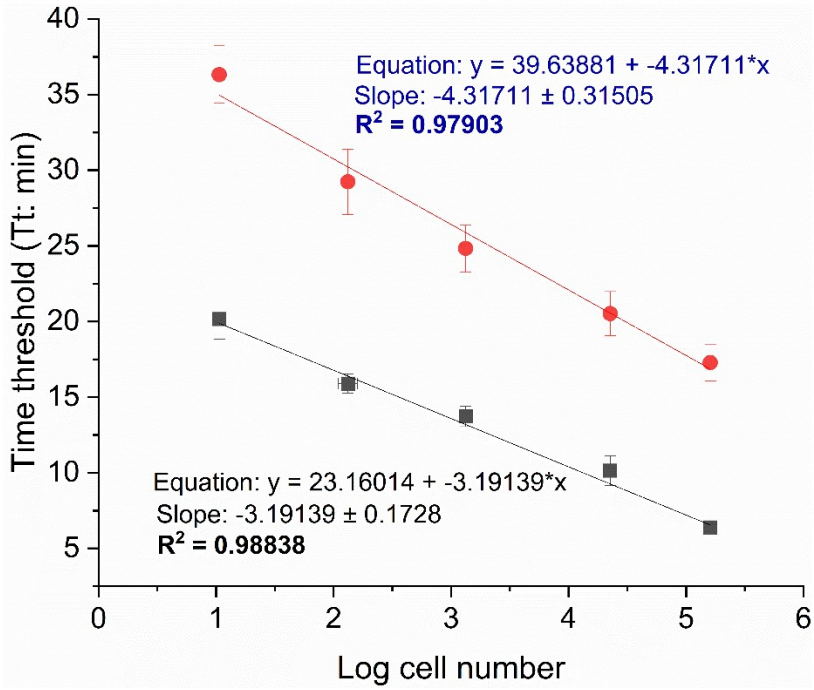

Supplementary Figure S5. Standard curve of the LAMPTRON system for quantifying *P. multistriata* cells in concentrations ranging from $1.6x10^5$ to $1.07x10^1$ cells/mL, as obtained using real-time fresh LAMP (black square) and vitrified preserved LAMP (red circle) methods. The data are expressed as the mean ± SM (standard error of the mean) of at least 3 independent samples for each standard concentration. The insets show slopes, intercepts, and correlation coefficients (R^2) of linear regression of data for fresh LAMP (represented by the black text below the graph) and vitrified preserved reagents (represented by the blue text above the graph).

S7. Reproducibility of LAMPTRON modules

This section supports the reliability of the LAMPTRON analyser, including both extraction and amplification modules, by demonstrating consistent DNA purification and amplification results across independent experiments and reagent batches.

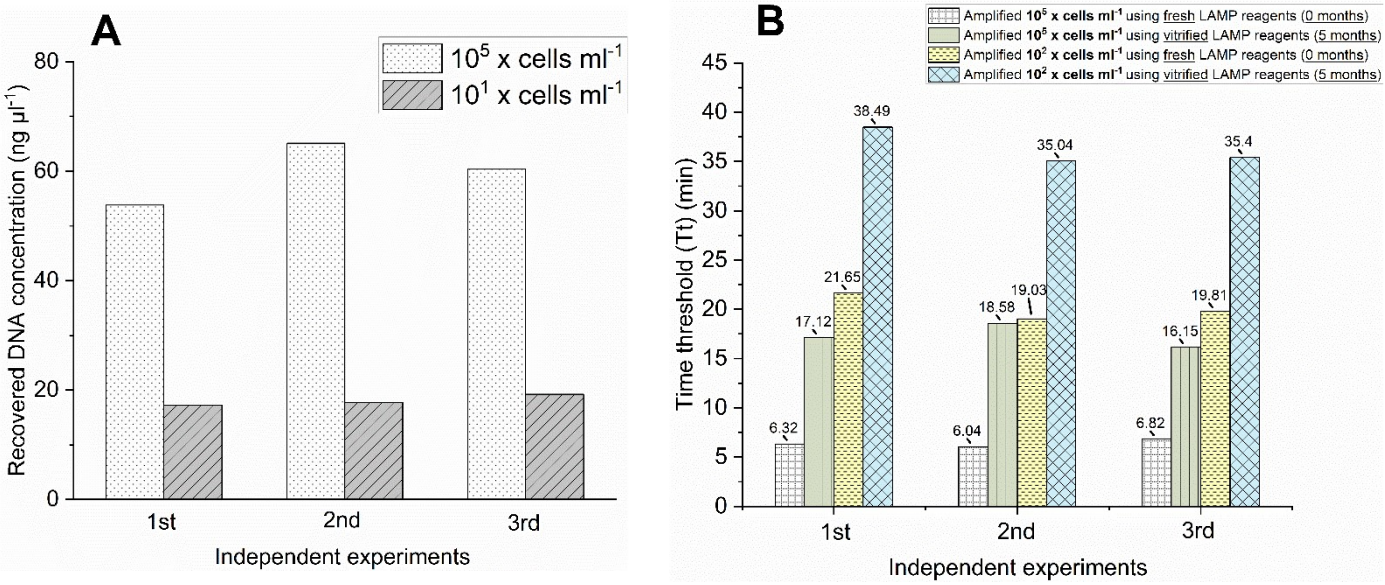

Supplementary Figure S6. Reproducibility of DNA purification and fluorescence measurements by the LAMPTRON analyser. A) Comparison of the quantity of the DNA isolated from $1.6x10^5$ and $1.07x10^1$ *P. multistriata* cells per mL from three independent experiments. B) The changes of T_t values of both *P. multistriata* cell numbers using both freshly prepared and pre-stored vitrified LAMP assays (5-month shelf-life) that were obtained by three independent experiments on the LAMPTRON system.

Part III: Microfluidic Hardware and Electronics

S8. Optimisation of the microfluidic design

To optimise the functionality of the LAMPTRON chip, we evaluated various channel dimensions and microchamber geometries to ensure laminar fluid flow and limited carryover between solutions. To do this, we employed COMSOL Multiphysics 5.5 software to simulate fluid flow in a 3D geometrical model of an extraction microchamber packed with silica beads. Initially, we investigated the potential challenge of bead slurry aggregation in microchannels which could block fluid flow and delay reagent flushing during the extraction process. [22] Simulation results using COMSOL demonstrated that the bead-packed reservoir remained structurally stable, and steady laminar flow was observed under current microchannel dimensions and operating conditions, as summarised in section 2.2 of the main article. The resulting Reynolds number (Re) was below the threshold of 2300, allowing for steady laminar flow through the bead-packed microchamber. [23] Another functional limitation we investigated was the resistance to the fluid flow caused by packed glass beads in

329 microchannels, which could resist the fluid flow and lead to backpressure, as demonstrated

330 in similar bead-based systems. [24, 25] This backflow could lead to a carryover of extraction

331 reagents, inhibiting amplification reactions and impeding the automated DNA extraction

process. [26] The simulation results shown in Figure S7-A indicate a steady velocity field that

333 maintains the concentration profile through beads immobilised on the bed of the extraction

chamber, ensuring high DNA binding. In bench-top testing, sustained fluid retention was

335 achieved by positioning solenoid valves at both the inlet and outlet of the detection

336 microchamber, effectively preventing backflow that could lead to contamination or inhibit

the LAMP reaction. By opening these valves and operating the syringe pump, the eluted DNA was titrated to rehydrate the vitrified LAMP reagents that were previously manually loaded into the detection chamber. LAMP products were detected via a small and compact fluorescence unit (FluoSens, QIAGEN GmbH, Hilden, Germany) aligned directly beneath the reaction microchamber. The use of this miniaturised and compact fluorescence unit provides the advantages of simplicity, modest cost, and allows for quick and easy assembly with functional parts of the LAMPTRON prototype. As a result, the on-chip DNA extraction protocol and LAMP detection can be adapted into a semi-automated workflow.

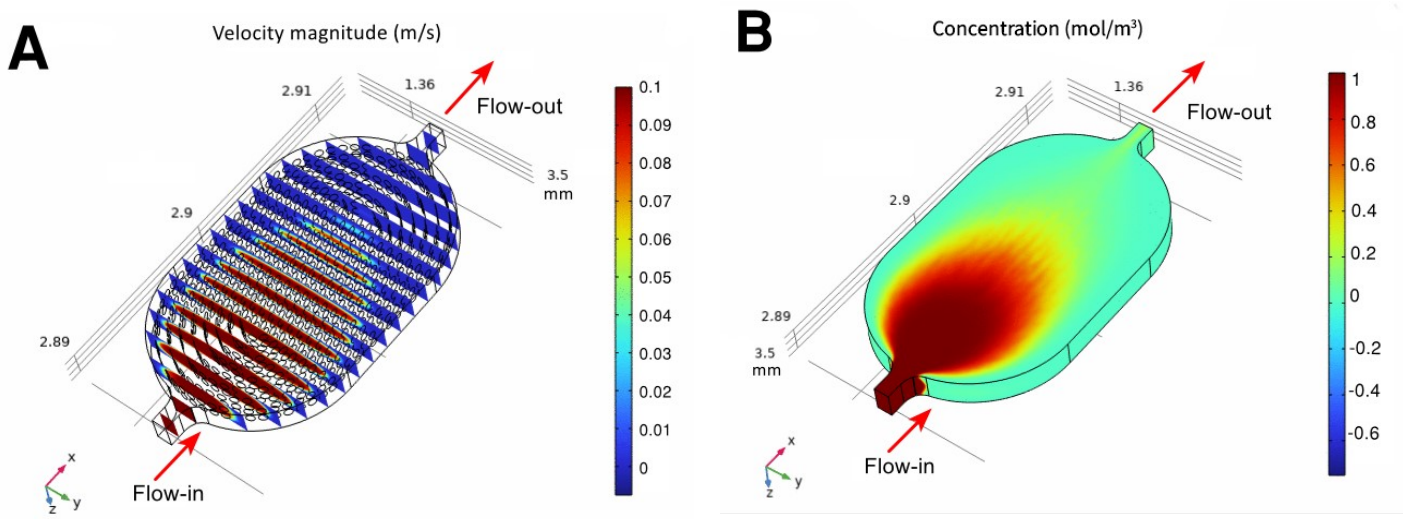

Supplementary Figure S7. Surface concentration and velocity profiles of DMA-DNA complexes (i.e., diluted species) within the extraction chamber packed with silica beads. The simulation illustrates a single-phase flow interface model incorporating the transport of diluted species. DMA-DNA complexes enter through the lower inlet, diffuse through the packed silica bead matrix, and exit via the outlet, revealing transport obstructions and flow heterogeneity within the microchamber.

S9. Autonomous pumping system

The incorporation of the pumping system represents a step towards demonstrating the autonomous operation capability of the LAMPTRON system. This pumping system has previously proved its utility in conducting *in-situ* chemical analyses at depths of up to 6,000 metres, as deployed in multiple oceanic locations by the Ocean Technology and Engineering Group (OTE) at the National Oceanography Centre. [27, 28] For the first time, this system has been adapted to process genomic samples, offering the potential for *in-situ* biological analyses in a wide array of environmental settings.

To enable autonomous operation, a revised version of the existing pumping system was developed, accommodating a configuration with four linked syringe pumps each equipped with solenoid valves (LFNA1250125H, Lee Co., United States), and ¼”-28 threaded outlets, as illustrated in Figure S8. This design allows for transitions between various pumping speeds within a single pumping cycle. The term "pumping cycle" here refers to the sequence of steps

involved in moving fluids through microchannels when the valve changes from a closed to an open state. [29] Most importantly, this design supports a pumping sequence that involves the individual loading of each DNA extraction reagent in its respective container, followed by transportation into channels, mixing with different fluids or components such as microbeads, or disposal into a waste container. This flexible pumping system enables the free exchange among extraction reagents, facilitating an automated on-chip DNA extraction process.

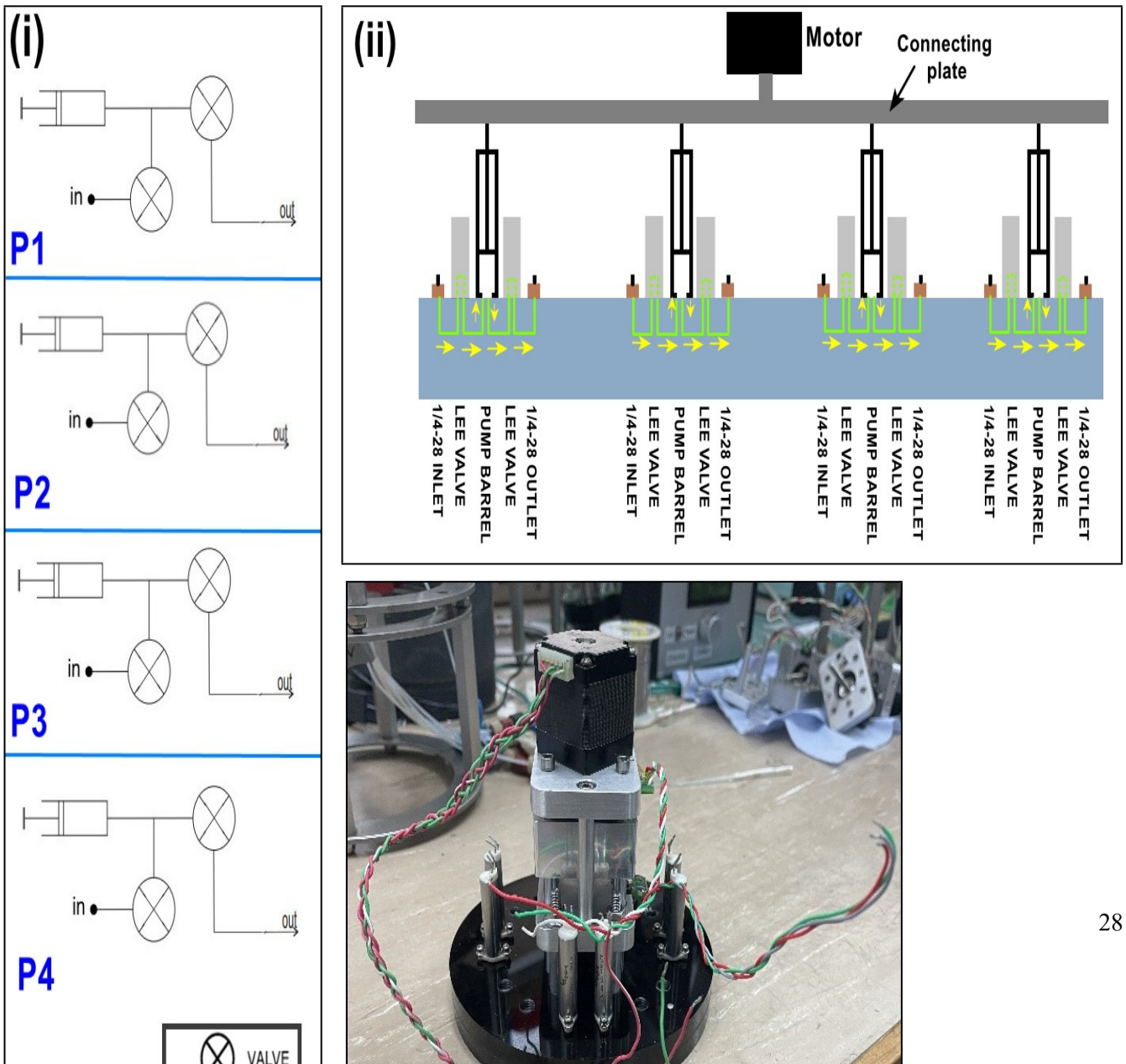

Supplementary Figure S8. Autonomous microfluidic pump system. i) A generic chip schematic demonstrating multiple individual fluidic routes, each connected to one of the four parallel syringe pumps (P1, P2, P3, and P4). ii) A schematic diagram shows the custom-made pumping system, which includes four syringe pumps, valves, and ¼”-28 outlets for each pump, all actuated by a Haydon Kerk Size 11 stepper motor linear actuator. iii) An image shows the setup of the valve-controlled selective routing.

S10. LAMPTRON prototype

This section shows the LAMPTRON prototype, highlighting its Arduino-based electronic control for heater regulation, temperature sensing, and data acquisition.

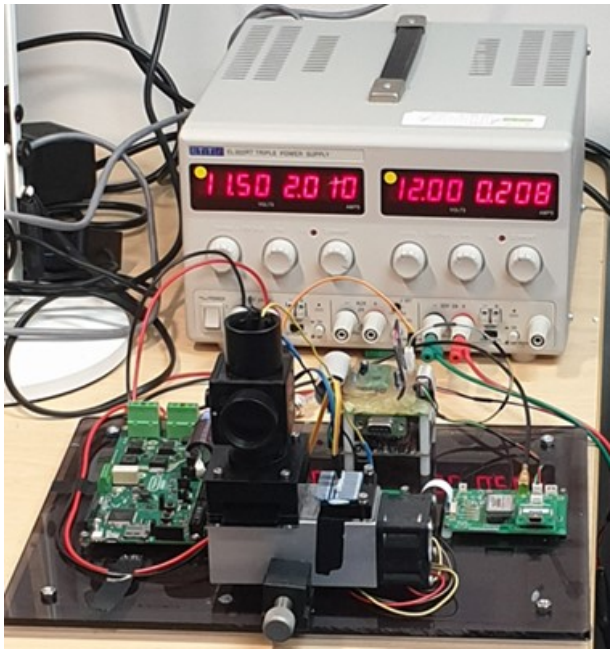

Supplementary Figure S9. The first prototype of LAMPTRON incorporated an Arduino circuit for electronic control of the heater, temperature sensor and data capture.

Part IV: Notes and references

1. R. Andersen, J. Berges, P. Harrison and M. Watanabe, *Algal Culture Techniques*, 2005, 429-539.
2. J. M. Newton, D. Schofield, J. Vlahopoulou and Y. H. Zhou, *Biotechnol Progr*, 2016, **32**, 1069-1076.
3. D. I. Walker, J. McQuillan, M. Taiwo, R. Parks, C. A. Stenton, H. Morgan, M. C. Mowlem and D. N. Lees, *Water Res*, 2019, **161**, 652-652.
4. K. Dilley, F. Pagan and B. Chapman, *Sci Justice*, 2021, **61**, 193-197.
5. H. Lee, C. Park, W. Na, K. H. Park and S. Shin, *Npj Precis Oncol*, 2020, **4**, 1-10.
6. B. Subeshan, A. Usta and R. Asmatulu, *Surf Interfaces*, 2020, **18**, 1-11.
7. J. K. Brunson, S. M. K. McKinnie, J. R. Chekan, J. P. McCrow, Z. D. Miles, E. M. Bertrand, V. A. Bielinski, H. Luhavaya, M. Obornik, G. J. Smith, D. A. Hutchins, A. E. Allen and B. S. Moore, *Science*, 2018, **361**, 1356-1358.
8. Z. Y. He, Q. Xu, Y. Chen, S. Y. Liu, H. Y. Song, H. Wang, C. P. Leaw and N. S. Chen, *Commun Biol*, 2024, **7**, 1-12.
9. Z. Y. Nie, X. P. Long, N. E. Bouroubi, H. C. Liu, S. T. Cao, Y. X. Chen, X. F. Zheng and J. L. Xia, *Curr Pharm Biotechno*, 2023, **24**, 599-610.
10. K. J. McLean and A. W. Munro, in *Encyclopedia of Signaling Molecules*, ed. S. Choi, Springer New York, New York, NY, 2016, pp. 1-18.
11. S. Hardardottir, S. Wohlrab, D. M. Hjort, B. Krock, T. G. Nielsen, U. John and N. Lundholm, *Bmc Mol Biol*, 2019, **20**, 1-14.
12. K. A. Lema, G. Metegnier, J. Quéré, M. Latimier, A. Youenou, C. Lambert, J. Fauchot and M. Le Gac, *Genome Biol Evol*, 2019, **11**, 731-747.
13. S. F. Altschul, W. Gish, W. Miller, E. W. Myers and D. J. Lipman, *J Mol Biol*, 1990, **215**, 403-410.
14. S. Basu, S. Patil, D. Mapleson, M. T. Russo, L. Vitale, C. Fevola, F. Maumus, R. Casotti, T. Mock, M. Caccamo, M. Montresor, R. Sanges and M. I. Ferrante, *New Phytol*, 2017, **215**, 140-156.
15. V. Di Dato, F. Musacchia, G. Petrosino, S. Patil, M. Montresor, R. Sanges and M. I. Ferrante, *Sci Rep-Uk*, 2015, **5**, 1-14.
16. M. A. Larkin, G. Blackshields, N. P. Brown, R. Chenna, P. A. McGettigan, H. McWilliam, F. Valentin, I. M. Wallace, A. Wilm, R. Lopez, J. D. Thompson, T. J. Gibson and D. G. Higgins, *Bioinformatics*, 2007, **23**, 2947-2948.
17. C. Camacho, G. Coulouris, V. Avagyan, N. Ma, J. Papadopoulos, K. Bealer and T. L. Madden, *Bmc Bioinformatics*, 2009, **10**, 1-9.
18. A. Marchler-Bauer, Y. Bo, L. Y. Han, J. E. He, C. J. Lanczycki, S. N. Lu, F. Chitsaz, M. K. Derbyshire, R. C. Geer, N. R. Gonzales, M. Gwadz, D. I. Hurwitz, F. Lu, G. H. Marchler, J. S. Song, N. Thanki, Z. X. Wang, R. A. Yamashita, D. C. Zhang, C. J. Zheng, L. Y. Geer and S. H. Bryant, *Nucleic Acids Res*, 2017, **45**, 200-203.
19. F. V. Shirshikov and J. A. Bespyatykh, *Russ J Bioorg Chem+*, 2022, **48**, 1159-1174.
20. K. Malpartida-Cardenas, L. Miglietta, T. Peng, A. Moniri, A. Holmes, P. Georgiou and J. Rodriguez-Manzano, *Sensors & Diagnostics*, 2022, **1**, 465-468.
21. G. J. Nixon, H. F. Svenstrup, C. E. Donald, C. Carder, J. M. Stephenson, S. Morris-Jones, J. F. Huggett and C. A. Foy, *Biomol Detect Quantif*, 2014, **2**, 4-10.
22. R. Zhong, D. Liu, L. Yu, N. Ye, Z. Dai, J. Qin and B. Lin, *Electrophoresis*, 2007, **28**, 2920-2926.
23. K. Benz, K. P. Jackel, K. J. Regenauer, J. Schiewe, K. Drese, W. Ehrfeld, V. Hessel and H. Lowe, *Chem Eng Technol*, 2001, **24**, 11-17.
24. R. D. Oleschuk, L. L. Shultz-Lockyear, Y. B. Ning and D. J. Harrison, *Anal Chem*, 2000, **72**, 585-590.
25. K. A. Wolfe, M. C. Breadmore, J. P. Ferrance, M. E. Power, J. F. Conroy, P. M. Norris and J. P. Landers, *Electrophoresis*, 2002, **23**, 727-733.

26. S. J. Reinholt and A. J. Baeumner, *Angew Chem Int Edit*, 2014, **53**, 13988-14001.
27. A. D. Beaton, A. M. Schaap, R. Pascal, R. Hanz, U. Martincic, C. L. Cardwell, A. Morris, G. Clinton-Bailey, K. Saw, S. E. Hartman and M. C. Mowlem, *ACS Sens*, 2022, **7**, 89-98.
28. M. Mowlem, A. Beaton, R. Pascal, A. Schaap, S. Loucaides, S. Monk, A. Morris, C. L. Cardwell, S. E. Fowell, M. D. Patey and P. Lopez-Garcia, *Front Mar Sci*, 2021, **8**, 1-15.
29. P. Woias, *Sensor Actuat B-Chem*, 2005, **105**, 28-38.